New constraints for low-momentum electronic excitations in condensed matter: fundamental consequences from classical and quantum dielectric theory

New constraints for low-momentum electronic excitations in condensed matter: fundamental consequences from classical and quantum dielectric theory

C T Chantler and J D Bourke

School of Physics, University of Melbourne, Parkville, Victoria 3010, Australia

E-mail: chantler@unimelb.edu.au

Abstract

We present new constraints for the transportation behaviour of low-momentum electronic excitations in condensed matter systems, and demonstrate that these have both a fundamental physical interpretation and a significant impact on the description of low-energy inelastic electron scattering. The dispersion behaviour and characteristic lifetime properties of plasmon and single-electron excitations are investigated using popular classical, semi-classical and quantum dielectric models. We find that, irrespective of constrained agreement to the well known high-momentum and high-energy Bethe ridge limit, standard descriptions of low-momentum electron excitations are inconsistent and unphysical. These observations have direct impact on calculations of transport properties such as inelastic mean free paths, stopping powers and escape depths of charged particles in condensed matter systems.

Keywords: electron dispersion, dielectric function, Bethe ridge, electron spectroscopy

(Some figures may appear in colour only in the online journal)

I. Introduction

The theory of dielectric response is critical to our understanding of optical and electronic interaction phenomena in condensed matter systems. From photo-absorption to electron scattering, to charge transportation, optical resonances and dynamical diffraction, robust dielectric modelling and computation is a key tool for quantification of the material properties that govern these interactions. While the fundamental physics required for these models has been established to high accuracy for several decades, applications of such models to real-world solids are still necessarily subject to a number of limiting approximations.

These approximations vary dramatically in scope and significance. For example, neglect of QED effects such as the vertex correction or the absence of fermionic exchange may not contribute significant errors in electron scattering theory in most practical situations [1]. Secondary excitation lifetimes and coupling between excitation channels, however, may contribute significantly for low-energy electron scattering (less than a few hundred electronvolts) while remaining relatively inconsequential for kiloelectronvolt electrons [2].

In this work we are concerned with approximations regarding the dispersion relations of electronic excitations in media with complex band structure—i.e. real world solids and other condensed matter systems. These approximations commonly arise in electron scattering models via the use of classical or semi-classical dielectric theories. Such theories are justified in the context of calculating bulk scattering properties by their formal agreement with quantum-mechanical models for the limiting cases of optical excitations (or, strictly speaking, excitations with zero momentum) [3] and excitations with very high momenta [4]. For finite low-momentum excitations, however, these models produce markedly different dispersion relations that impact directly upon the predicted velocity of collective and single-electron oscillators,

thus altering our conclusions regarding the transport behaviour of these particles.

Alternative models such as advanced density functional theory (DFT) using local density or *GW* approximations are similarly subject to a number of simplifications that become increasingly severe for continuum and finite-momentum excitations [5, 6]. Given that such calculations are becoming increasingly common in studies of electron transport phenomena [7, 8], it is important to investigate the physical and mathematical constraints that must be applied to assess the validity of their results.

In recent work investigating the lifetime broadening of low-energy electronic excitations [2], it was discovered that the quantum dielectric theory predicted a path of local minima in the broadening function corresponding to the dispersion relation of a non-relativistic classical free particle, $E = \frac{p^2}{2m}$. This feature persists in different materials and appears independent of the solid-state band structure. Here we elucidate the cause and physical significance of this feature, and demonstrate its significance by contrast with alternative models.

II. Generalised oscillator strength and the Bethe ridge

The basis of the dielectric theory is the complex dielectric function $\epsilon(q, \omega)$, corresponding to the ratio of the observed potential within a medium to the initial potential applied by some external field [9]. In the case of the external field produced by an incident energetic electron, it is convenient to present the energy loss function (ELF), defined as the imaginary component of the inverse of the dielectric function, i.e.
$\text{ELF} = \text{Im}\left[\frac{-1}{\epsilon(q, \omega)}\right]$.

This formulation is useful for the calculation of scattering properties, as the ELF is proportional to the matrix element for electronic transitions within the first Born approximation [10], and therefore can be considered as a relative probability for a medium to accept an excitation with energy $\hbar\omega$ and momentum $\hbar q$ [11]. The simplest example of this is for a nearly free electron gas (FEG) or jellium system. Within an FEG, there exists a single resonant frequency ω_p such that, in the limit $q \to 0$, the ELF becomes

$$\text{Im}\left[\frac{-1}{\epsilon(0, \omega)}\right]_\text{FEG} = \frac{\pi}{2}\delta(\omega - \omega_\text{p}). \qquad (1)$$

In a real medium, there may exist many excitation channels with varying relative probability amplitudes. We therefore write the ELF for a general material in terms of these excitation channels as

$$\text{Im}\left[\frac{-1}{\epsilon(0, \omega)}\right] = \sum_i A_i \text{Im}\left[\frac{-1}{\epsilon(0, \omega; \omega_\text{p} = \omega_i)}\right]_\text{FEG} \qquad (2)$$

where the values A_i are commonly known as *oscillator strengths*. For a material with a known overall charge density, the sum of these oscillator strengths is subject to a number of

causal constraints that are expressed by well known optical sum-rules [12, 13]. The oscillator strengths correspond to particular excitations characteristic of the absorbing material, and their magnitudes may be calculated using an appropriate implementation of DFT [14].

When the ELF is expressed in the limit $q \to 0$, it is said to exist in the optical limit, as the momentum of an optical excitation is very small relative to that of most electronic excitations. Accordingly, it is common to refer to $\text{Im}\left[\frac{-1}{\epsilon(0, \omega)}\right]$ as the optical ELF, or the optical oscillator strength (OOS) [15]. The complete ELF with explicit *q* dependence is then referred to as the generalised oscillator strength (GOS) [16].

The relationship between the OOS and the GOS is dependent upon the explicit *q*-dependent form of each oscillator *i*. Each optical oscillator will translate to a generalised oscillator following a dispersion equation defining the relationship between its energy and momentum. In general, this relationship may be modulated by the lifetime broadening of each oscillator, or by the interactions between oscillators. However, such modulations normally are considered to be very weak [2] or are neglected entirely [17, 18]. As the momentum of each oscillator is increased, its strength will correspondingly decrease due to the extension of optical sum-rules to higher momentum states [19].

The behaviour of the oscillators at very high momenta is dictated by the constraint that they act like classical particles in the limit $q \to \infty$. Indeed, regardless of the model employed, the (non-relativistic) dielectric behaviour of a single electron at rest is defined by a delta oscillator existing along the path $\omega = \frac{\hbar q^2}{2m}$ for all energies [20]. For a many-electron material, this behaviour will only exist at high momenta, and the form of the ELF will be broadened in an asymmetric fashion due to the electronic band structure [16].

This high-momentum limit is commonly known as the Bethe ridge, as it appears as a ridge-like structure in plots of the GOS, which historically have been known as the Bethe surface [21]. It was originally documented as early as 1930 [22], and has since been used extensively to guide and constrain dielectric models. Many models that exhibit the Bethe ridge at high momenta, and match the OOS at $q = 0$, have historically been considered sufficient for tabulations of electron inelastic mean free paths (IMFPs) and stopping powers, as only long-range integrals of the GOS are required to determine these material properties [23–25]. Recent work has shown that the dispersion relation at intermediate momenta can, however, have a significant impact for low-energy tabulations [26, 27], and moreover the choice of dielectric modelling has a much more significant impact on the fundamental understanding of the transport properties of bound excitations.

III. Dispersion of electronic excitations

To describe the dispersion of electronic excitations that make up the ELF, or GOS, the simplest option is to take a purely classical view. In this case the energy of the excitation is

simply set to its resonant energy plus an offset from the square of its momentum, yielding

$$\omega_q = \omega_i + \alpha \frac{\hbar q^2}{2m} \qquad (3)$$

where ω_q is the energy of the ith oscillator at momentum $\hbar q$. This dispersion relation was routinely used in early work with optical data models of dielectric response, with the α parameter set to unity to ensure agreement with classical physics at high momenta, and convergence to the Bethe ridge. Some modern works have used alternative values of α to test electronic behaviour at intermediate momenta [7, 18]; however, these may only represent physical models if α converges to 1 in the limit $q \to \infty$ (e.g. as in [28]).

An alternative to this classical dispersion relation is a semi-classical equation in order to improve agreement with the quantum theory near the optical limit. In this case a quartic relation is commonly used:

$$\omega_q^2 = \omega_i^2 + \beta v_F^2 q^2 + \left(\frac{\hbar q^2}{2m} \right)^2 \qquad (4)$$

where v_F is the Fermi velocity, calculated for each resonant oscillator in terms of its energy in the optical limit,

$$v_F = \frac{\hbar}{m} \left(\frac{3\pi^2 m \omega_i^2}{e^2} \right)^{1/3}. \qquad (5)$$

The β parameter is most often set equal to 1/3, enforcing agreement with Thomas–Fermi theory for low-momentum excitations [29, 30]. Such a formulation is most notably employed in the IMFP tabulations of Tanuma, Powell, and Penn for energies above 330 eV [31]. In other work, a β value of 3/5 is suggested [32], and we will consider both options in this analysis.

Quantum dielectric theory is significantly more complex and does not lend itself to a simple expression for the dispersion relation of electronic excitations. Nonetheless a dispersion function may be mapped by following the theory of Lindhard [33], which provides a dielectric function $\epsilon(q, \omega)$ explicitly in terms of the energy and momentum transfer as follows:

$$\epsilon(q, \omega) = 1 + \frac{4\pi e^2}{q^2} \sum_{\mathbf{k}} \frac{f^0(\mathbf{k}) - f^0(\mathbf{k} + \mathbf{q})}{E(\mathbf{k} + \mathbf{q}) - E(\mathbf{k}) - \hbar\omega}. \qquad (6)$$

Here the summation is over initial states in the absorbing material of momenta $\mathbf{k}$, with $f^0(\mathbf{k})$ being their energy distribution. Taking $f^0(\mathbf{k})$ as the Fermi distribution and integrating over momenta yields the well known result

$$\epsilon_L(q, \omega) = 1 + \frac{3\omega_p^2}{q^2 v_F^2} f \qquad (7)$$

where

$$f = \frac{1}{2} + \frac{1}{8z} [1 - (z-u)^2] \ln \left[\frac{z-u+1}{z-u-1} \right]$$
$$+ \frac{1}{8z} [1 - (z+u)^2] \ln \left[\frac{z+u+1}{z+u-1} \right]. \qquad (8)$$

This is expressed in term of dimensionless parameters z and u, which are given by

$$u = \frac{\omega}{q v_F}, \quad z = \frac{q}{2 q_F}. \qquad (9)$$

The use of the Lindhard dielectric function for individual oscillators of plasma frequency ω_p enables a quantification of the peak energy in the Bethe surface at different values of momentum, and hence a determination of ω_q from the quantum theory. This formulation explicitly neglects excitation broadening, which may only be included in a physical fashion by the extension of the Lindhard function to a Mermin function [34]:

$$\epsilon_M(q, \omega) = 1 + \frac{(1 + i\gamma/\omega)[\epsilon_L(q, \omega + i\gamma) - 1]}{1 + (i\gamma/\omega)[\epsilon_L(q, \omega + i\gamma) - 1]/[\epsilon_L(q, 0) - 1]}. \qquad (10)$$

The parameter γ defines the lifetime broadening of each oscillator. Its value has a weak impact on the form of the dispersion relation ω_q, which reduces to that of the Lindhard theory when $\gamma = 0$.

IV. Group velocity and the electron inelastic mean free path

The form of the dispersion relation $\omega_q = f(q, \omega_i)$ can be expressed in terms of the group velocity of an excitation $v(q, \omega_q) = \frac{\partial \omega_q}{\partial q}$, or loosely the propagation velocity of a pulse. In the case of lossless oscillators (i.e. where $\gamma_i = 0$) this velocity is sufficient to uniquely define the ELF for all energies and momenta, as it determines the energy–momentum relationship of each excitation channel, while the relative amplitudes of oscillators are ideally constrained by optical sum-rules. For oscillators of finite lifetime ($\gamma_i > 0$), the ELF is also affected by the characteristic shape of the oscillators, which may be of the Mermin type, the Drude type, or some other model [19].

One of the most direct practical applications of the electron ELF is in the determination of the electron inelastic mean free path (IMFP). Due to the physical interpretation of the ELF as a mapping of excitation probabilities, the IMFP $\lambda(E)$ may be evaluated directly via an integral over the ELF with appropriate kinematic limits [35]. This has been performed using a number of model formulae and dielectric functions [17, 27, 31], and here we explicitly consider our recent self-consistent formulation given by [2]

$$\lambda(E)_N^{-1} = \frac{\hbar}{a_o \pi E} \int_0^{\frac{E - E_F}{\hbar}} \int_{q_-}^{q_+} \int_0^\infty \frac{2}{\pi} \frac{\omega'}{q}$$

$$\times \mathrm{Im} \left[\frac{-1}{\epsilon_{data}(0, \omega')} \right]$$

$$\times \mathrm{Im} \left[\frac{-1}{\epsilon_M(q, \omega, \gamma_i(q)_{N-1}; \omega_p = \omega')} \right] \mathrm{d}\omega' \mathrm{d}q \mathrm{d}\omega \qquad (11a)$$

$$\gamma_i(q)_N = \hbar \frac{\mathrm{d}\omega_q}{\mathrm{d}q} \bigg|_{\omega_q, q} \lambda(E)_N^{-1} \Theta(N - \delta). \qquad (11b)$$

This formula is a generalised version of the classic Penn algorithm [1], and is self-consistent via iterations of the excitation broadening function $\gamma_i(q)$. It takes a known optical ELF (or OOS—$\mathrm{Im}\left[\frac{-1}{\epsilon_{\mathrm{data}}(0, \omega')}\right]$) from some external source, such as DFT or experiment, and generalises it to a momentum-dependent ELF (GOS) using Mermin functions. In the first iteration, $N = 1$ and $\gamma_i(q) = 0 \, \forall \, i, q$, meaning that a lossless system is modelled and the ELF, and hence IMFP, is directly modulated by the group velocity $\frac{\partial \omega_q}{\partial q}$. For higher iterations, the group velocity still determines the evolution of the peaks in the Mermin term—$\mathrm{Im}\left[\frac{-1}{\epsilon_{\mathrm{M}}(q, \omega, \gamma_i(q)_{N-1}; \omega_p = \omega_i)}\right]\mathrm{d}\omega'\mathrm{d}q\mathrm{d}\omega$—but also directly modulates the broadening function. The IMFP is especially sensitive to this broadening for electron energies below 100 eV where plasmon resonances are dominant, as has been recently demonstrated by our group [26] and others [11, 36]. It is therefore instructive to consider the behaviour and physicality of the group velocity within different dielectric models in order to elucidate the fundamental cause of variations in calculated electron scattering parameters.

V. Excitation broadening and the velocity surface

The excitation broadening function $\gamma_i(q)$ has also been found to have interesting and significant behaviour from the recent IMFP study involving coupled plasmons [2]. This function, inversely proportional to the lifetime of excitations as a function of energy and momentum (equation (11*a*)), was found to possess local minima following the classical free-electron dispersion relation.

The broadening function is proportional to the product of the group velocity of an individual excitation and the inverse of its IMFP: λ^{-1}. These functions are illustrated for the case of molybdenum in figure 1 using the quantum dielectric theory employed in [2]. The key features corresponding to maximum and minimum broadening clearly arise from the form of the group velocity surface, rather than the inverse IMFP. Therefore local maxima in the group velocity of an excitation correspond to lifetime minima, and vice versa.

Figure 1 is plotted in terms of the energies and momenta of the excitations; however, care must be taken to interpret the energy axis. The values in the figure correspond to a given amount of momentum $\hbar q$ having been transferred to a resonant excitation with an optical frequency ω_i. This is why the momentum axis is not bounded. If one wishes to plot, for example, the group velocity of an excitation in terms of its energy and momentum directly, then the energy axis becomes $\hbar \omega_q$ and the momentum becomes bounded by the classical limit $q = \sqrt{\frac{2m\omega_q}{\hbar}}$. This kind of plot is shown in figure 2.

In this work we will interpret the results of the quantum and semi-classical theories in terms of $\hbar \omega_i$ (e.g. figure 1), as this view lends itself more directly to a physical analysis of the validity of each. It is also convenient to treat both the quantum and semi-classical group velocities (v_{q} and v_{sc}) in terms of their deviations from the classical velocity $v_{\mathrm{c}} = \hbar q/m$. These functions, $v_{\mathrm{sc}} - v_{\mathrm{c}}$ and $v_{\mathrm{q}} - v_{\mathrm{c}}$, are plotted in figure 3. Here we
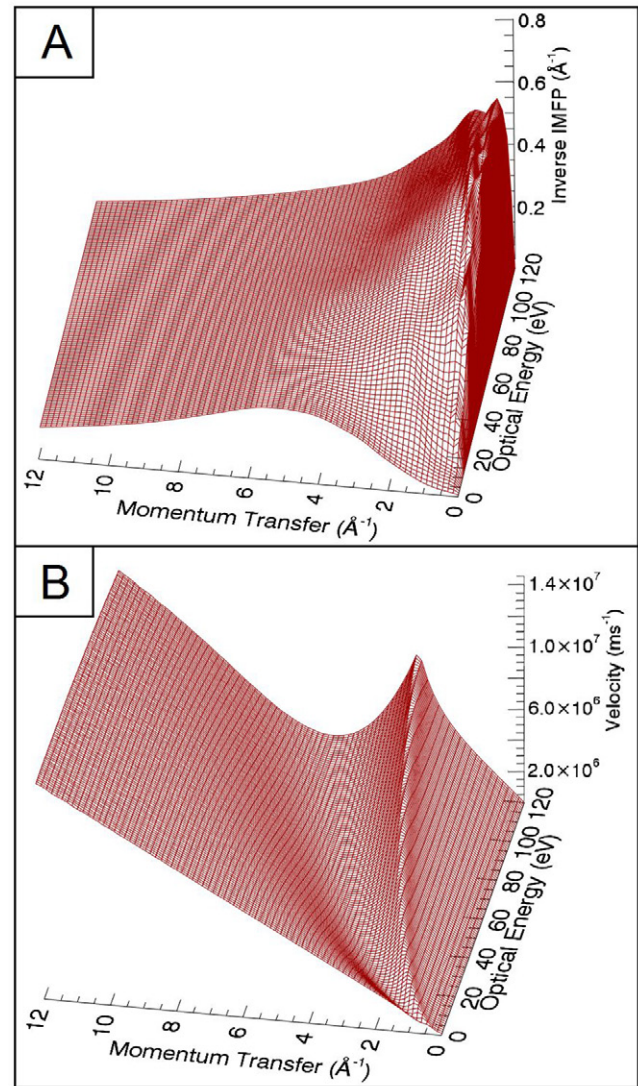
Figure 1. Components of the broadening function for electronic excitations in a solid—(A) the inverse IMFP and (B) the group velocity using quantum theory. The functions are represented in terms of the momenta $\hbar q$ of the excitations, and their 'optical' energies $\hbar \omega_i$. The quantum mechanical minimum is seen to derive from the group velocity.

use the two literature values for the semi-classical β parameter ($\frac{1}{3}$ and $\frac{3}{5}$), equation (4), and the quantum Lindhard and Mermin theories with γ equal to zero and 10 eV, respectively (equations (7) and (10)).

The classical theory produces a flat surface with velocity directly proportional to momentum. However, the semi-classical and quantum theories produce characteristic features in the velocity surface at low momentum values. The quantum theories produce clear paths of local minima, which when viewed on an absolute scale precisely follow the classical dispersion line $\omega_i = \frac{\hbar q^2}{2m}$. These regions correspond to maximum-lifetime, or maximally stable, excitation states for a condensed matter system. In addition, the quantum theories further predict an analogue path corresponding to a maximum velocity/minimum lifetime at lower momenta (the ridges in
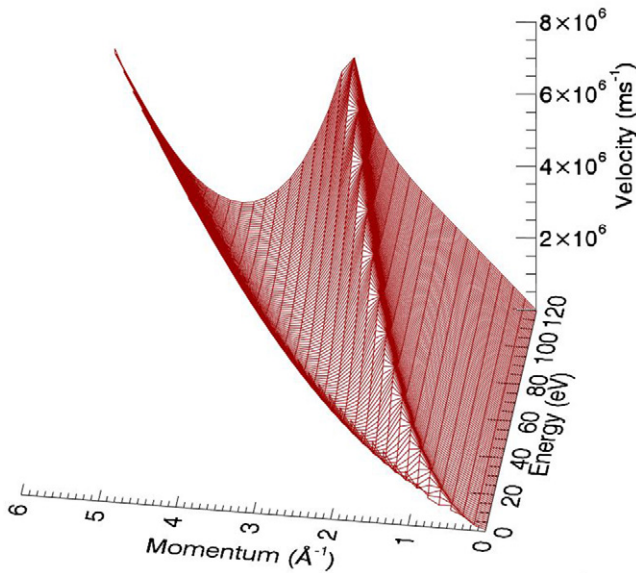
Figure 2. The group velocity of excitations in a condensed matter system $\frac{\partial \omega_q}{\partial q}$, as a direct function of the energy of the excitation $\hbar \omega_q$ and its momentum $\hbar q$ using quantum theory. The momenta are constrained by an upper bound corresponding to the dispersion relation of a free particle.

the corresponding plots). The strength of these features is diminished as excitation broadening is introduced; however, their positions are not affected so long as the broadening coefficient γ is greater than the optical excitation energy ω_i.

The semi-classical theories feature either positive or negative deviations from the classical result, depending on the value of the β parameter, but these deviations do not produce local minima or maxima on an absolute scale. The semi-classical velocities do, however, match the classical and the quantum results in the limits $q = 0$ and $q \rightarrow \infty$.

VI. Significance

It may come as some surprise that superficially these velocity surfaces possess such radically different forms. However, one should note that the semi-classical quartic equation (equation (4)) is a simple generalisation of the classical quadratic dispersion, with only an adjustment to the coefficient of the q^2 term. The value of $\beta - \frac{\hbar \omega_i}{m v_F^2}$ determines the shape of the semi-classical velocity surface, with values greater than zero leading to a maximum relative to the classical result, and values less than zero leading to a minimum. A surface similar to the quantum result with both maxima and minima would demand a higher-order dispersion relation.

It is not possible to reproduce the minimal path from the quantum theory with local turning points following the free particle dispersion relation by using a semi-classical equation such as that of equation (4). One may define a path of local minima (or maxima) relative to the classical result by adjusting β; however, as this path approaches $\omega_i = \frac{\hbar q^2}{2m}$, β approaches $\frac{\hbar \omega_i}{m v_F^2}$ and the depth of the minima approaches zero.

The case where $\beta = 1/3$ is comparatively close to this condition, especially for high values of ω_i.

The existence of a well defined trench in the quantum velocity surface is important as it represents a maximally stable state of excitation that is largely material independent. The detailed band structure of the material will then determine the cross section for transitions into this excited state. The state is not one with a free-energy dispersion relation, as such states are constrained to match the classical result, but rather corresponds to a state in which momentum is deposited into a plasmon resonance with corresponding energy $\omega_i = \frac{\hbar q^2}{2m}$ in the optical limit. In this instance a small amount of energy will also be deposited, and so the final energy $\hbar \omega_q$ will be slightly higher than $\hbar \omega_i$. The dispersion relations for these maximally stable excitations are shown in figure 4 relative to both ω_i and ω_q.

The phenomenon of minimum values in the velocity surface also has significant impact on the direct evaluation of the energies absorbed by resonant excitations using the different theoretical models. The velocity and momentum of an excitation are related to this energy via the canonical equation $\frac{\partial \mathscr{H}}{\partial p} = v$, which we can also write as

$$E = \hbar \int_0^q v \, \mathrm{d}q' \tag{12}$$

where this relationship is to be taken as a definition for a general excitation. The actual energy of a low-momentum excitation is strongly affected by its interaction with its environment. Within the quantum model, the velocity is determined primarily by the resonant optical energy of the excitation ω_i modulated by coupling to alternative excitation channels via broadening [2]. As momentum is added to the excitation, however, its properties must become more classical, leading to the condition

$$\lim_{q \rightarrow \infty} \int_0^q v \, \mathrm{d}q' = \frac{\hbar q^2}{2m} \tag{13}$$

which must be satisfied by any dielectric theory in accordance with the correspondence principle. Inspection of figure 3 and consideration of the previous discussion on quartic dispersion relations clearly shows that the semi-classical theory does not satisfy this condition, except for the trivial case where it reduces identically to the classical quadratic dispersion. The quantum-mechanical Lindhard model, however, has been shown numerically to converge to the correct result. This holds true even with the generalisation to a Mermin function and inclusion of a constant broadening term γ.

VII. Conclusions

It is clear that the energy condition of equation (13) must be satisfied for any valid theory, in addition to the Bethe ridge constraint, and most probably the existence of a velocity minimum along the free-particle dispersion path. The classical modelling (equation (3)) can match the first two conditions depending on the form of α, but does not predict the minimum
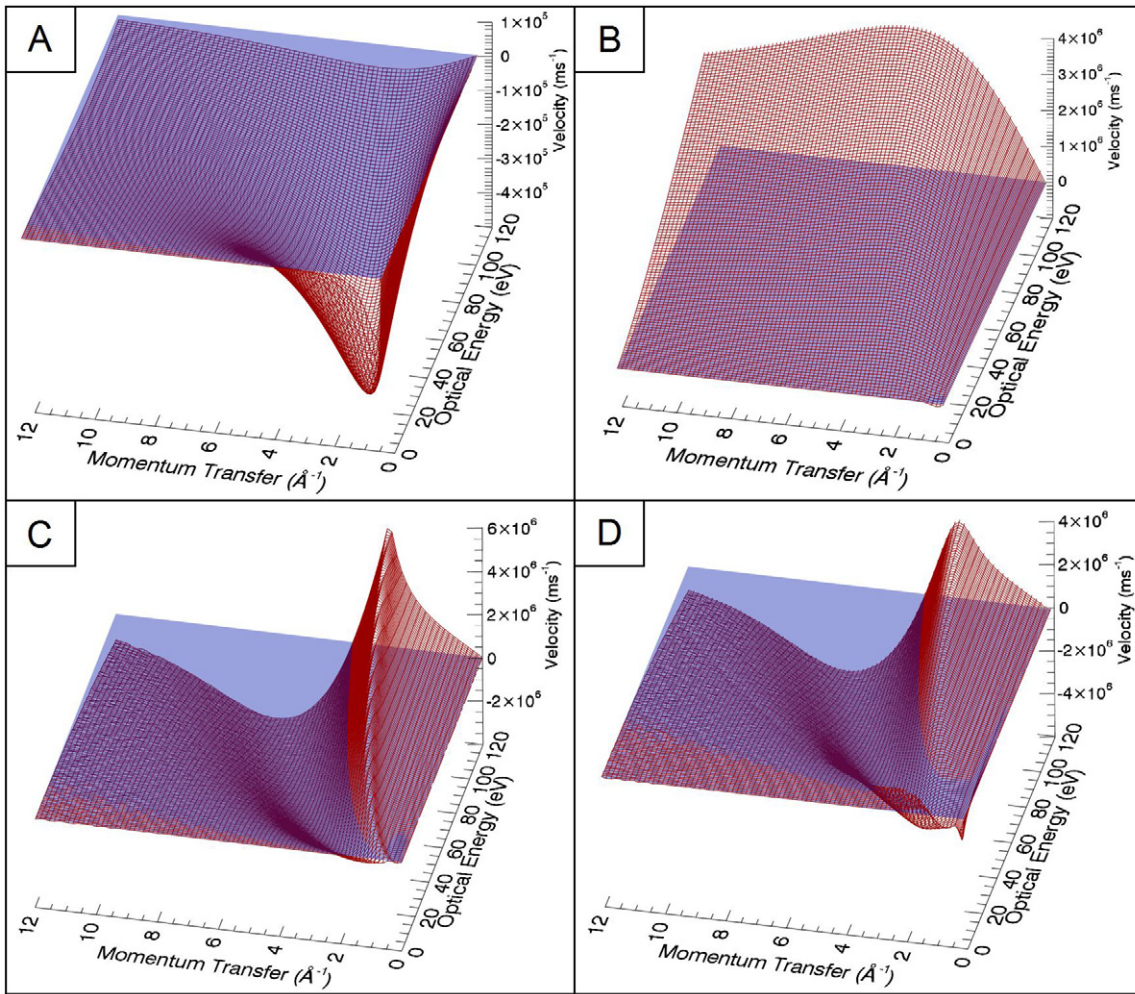
Figure 3. The group velocity of excitations in a condensed matter system as determined by (A) semi-classical theory using $\beta = 1/3$, (B) semi-classical theory using $\beta = 3/5$ (equation (4)), (C) the quantum theory of Lindhard (equation (7), $\gamma = 0$) and (D) the quantum theory of Mermin (equation (10), $\gamma = 10$ eV). The plotted values are the differences from the classical theory v_c, included for reference as the flat blue zero planes.

in the velocity surface. The Bethe ridge condition requires only that equation (3) must have $\alpha \to 1$ as $q \to \infty$: that is, α is not a constant unless it is precisely unity. If it is a variable, then it must also average to unity in order to conserve energy.

The semi-classical forms actually perform worse than their classical analogues. Although they adhere to the Bethe ridge constraint, they neither conserve energy nor predict the velocity minima irrespective of the choice of β. The Lindhard and Mermin formalisms, however, exhibit the correct behaviour, and notably do so regardless of the broadening of excitation channels, making them valid forms for a self-consistent scattering theory such as that expressed by equation (11).

Although the Bethe ridge constraint has long been used to assess dielectric theories, this is the first time that a variety of models have been assessed in terms of the energy condition and velocity minima. It has been shown extensively that alternative theories with different dispersive behaviour lead to significantly different scattering coefficients [24, 31, 37], but they have not previously been robustly interrogated to demonstrate the underlying physical basis of their predictions. Given the new evidence presented here, there is a strong case

for the abandonment of the currently prevalent classical and semi-classical models, and for the careful consideration of any proposed variation of the Lindhard and Mermin models of dielectric response. This discussion does not strictly prove the validity or unique applicability of the Lindhard and Mermin forms, but it does confirm that they follow appropriate and expected quantum behaviour. The comparison of Lindhard, Mermin and possible alternative forms invites further investigation.

These new constraints are also relevant to models which may consider the behaviour of collective (plasmon) excitations and single-electron excitations separately. Recent work using density functional theory has suggested that these different kinds of excitation may exhibit markedly different dispersion relations [38], potentially due to a different level of modulation from the band structure of the material for intraband and interband excitations [14]. If this is so, then such relations will need to be quantified with respect to their momentum- and energy-dependent velocities, i.e. the velocity surface. These quantities will be subject to the same constraints elucidated here, and so this treatment will act as a critical test of the validity of these theories.
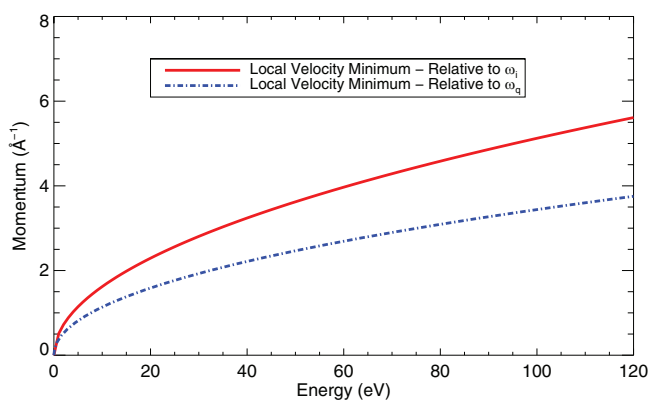
Figure 4. Local minima of the group velocity (local maxima of the lifetime) using quantum theory in terms of both ω_i and ω_q. In terms of ω_i, the result corresponds to the dispersion of a classical free particle.

The velocity surface itself is a measurable physical quantity in a similar fashion to the electron ELF. Surface technologies such as reflection electron energy loss spectroscopy (REELS) can currently measure momentum-dependent loss functions [39], the peaks of which may be traced to derive the dispersive behaviour of individual excitations [38]. Other physical quantities evaluated from the same measurements, such as stopping powers and differential inverse IMFPs (DIIMFPs), are similarly sensitive to the velocity surface for excitations in the material. A detailed understanding of the behaviour of both single-electron and plasmon excitations will be critical to improvements in accurate analysis and interpretation of these experiments and to the interpretation of fundamental electron scattering properties in general condensed matter systems.

Acknowledgments

References

[1] Penn D R 1987 *Phys. Rev.* B **35** 482
[2] Bourke J D and Chantler C T 2015 *J. Phys. Chem. Lett.* **6** 314
[3] Chen Y F, Kwei C M and Tung C J 1993 *Phys. Rev.* B **48** 4373
[4] Tanuma S, Powell C J and Penn D R 1991 *Surf. Interface Anal.* **17** 911
[5] Parr R G 1983 *Annu. Rev. Phys. Chem.* **34** 631
[6] Hebert C 2007 *Micron* **38** 12
[7] Werner W S M, Glantschnig K and Ambrosch-Draxl C 2009 *J. Phys. Chem. Ref. Data* **38** 1013
[8] Chantler C T and Bourke J D 2014 *J. Phys. Chem.* A **118** 909
[9] Ziman J M 1972 *Principles of the Theory of Solids* 2nd edn (Cambridge: Cambridge University Press)
[10] Nikjoo H, Uehara S and Emfietzoglou D 2012 *Interaction of Radiation with Matter* (Boca Raton, FL: CRC Press)
[11] Denton C D, Abril I, Garcia-Molina R, Moreno-Marin J C and Heredia-Avalos S 2008 *Surf. Interface Anal.* **40** 1481
[12] Smith D Y and Shiles E 1978 *Phys. Rev.* B **17** 4689
[13] Barkyoumb J H and Smith D Y 1990 *Phys. Rev.* A **41** 4863
[14] Ambrosch-Draxl C and Sofo J O 2006 *Comput. Phys. Commun.* **175** 1
[15] Fernandez-Varea J M, Salvat F, Dingfelder M and Liljequist D 2005 *Nucl. Instrum. Methods* B **229** 187
[16] Segui S, Dingfelder M, Fernandez-Verea J M and Salvat F 2002 *J. Phys. B: At. Mol. Opt. Phys.* **35** 33
[17] Sorini A P, Kas J J, Rehr J J, Prange M P and Levine Z H 2006 *Phys. Rev.* B **74** 165111
[18] Vos M and Grande P L 2014 *Surf. Sci.* **630** 1
[19] Chantler C T and Bourke J D 2014 *Phys. Rev.* B **90** 174306
[20] Fano U 1963 *Annu. Rev. Nucl. Sci.* **13** 1
[21] Inokuti M 1971 *Rev. Mod. Phys.* **43** 297
[22] Bethe H 1930 *Ann. Phys.* **5** 325
[23] Ding Z-J and Shimizu R 1989 *Surf. Sci.* **222** 313
[24] Kwei C M, Chen Y F, Tung C J and Wang J P 1993 *Surf. Sci.* **293** 202
[25] Ashley J C 1990 *J. Electron Spectrosc. Relat. Phenom.* **50** 323
[26] Bourke J D and Chantler C T 2012 *J. Phys. Chem.* A **116** 3202
[27] Da B, Shinotsuka H, Yoshikawa H, Ding Z J and Tanuma S 2014 *Phys. Rev. Lett.* **113** 063201
[28] Emfietzoglou D, Cucinotta F A and Nikjoo H 2005 *Radiat. Res.* **164** 202
[29] Lundqvist B I 1967 *Phys. kondens. Materie.* **6** 206
[30] Spruch L 1991 *Rev. Mod. Phys.* **63** 151
[31] Tanuma S, Powell C J and Penn D R 2011 *Surf. Interface Anal.* **43** 689
[32] Ritchie R H and Howie A 1977 *Phil. Mag.* **36** 463
[33] Lindhard J 1954 *Dan. Mat. Fys. Medd.* **28** 1
[34] Mermin N D 1970 *Phys. Rev.* B **1** 2362
[35] Tung C J, Ashley J C and Ritchie R H 1979 *Surf. Sci.* **81** 427
[36] Abril I, Garcia-Molina R, Denton C D, Perez-Perez F J and Arista N R 1998 *Phys. Rev.* A **58** 357
[37] Bourke J D, Chantler C T and Witte C 2007 *Phys. Lett.* A **360** 702
[38] Alkauskas A, Schneider S D, Hebert C, Sagmeister S and Draxl C 2013 *Phys. Rev.* B **88** 195124
[39] Vos M 2013 *J. Electron Spectrosc. Relat. Phenom.* **191** 65